AD-A159 101 EARLY TRANSONIC IDEAS IN THE LIGHT OF LATER DEVELOPMENTS(U) RENSSELAER POLYTECHNIC INST TROY NY DEPT OF MATERIALS ENGINEERING J D COLE 06 AUG 85 1/1

UNCLASSIFIED AFOSR-TR-85-0694 AFOSR-82-0155 F/G 20/4 NL

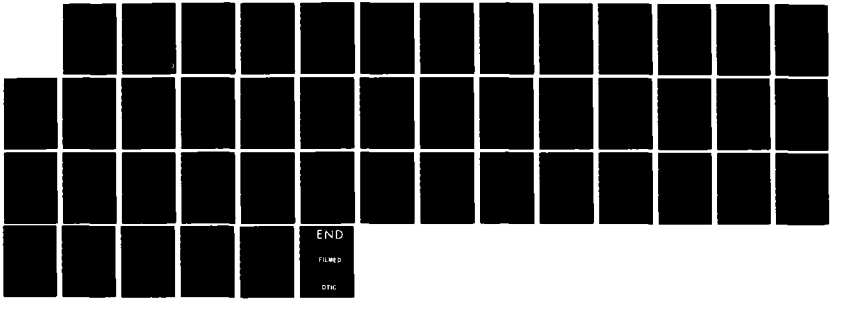

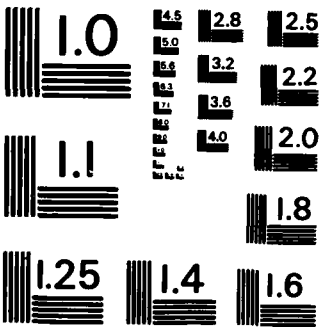

Uhclassified

SECURITY CLASSIFICATION OF THIS PAGE (When Data Entered)

REPORT DOCUMENTATION PAGE

READ INSTRUCTIONS BEFORE COMPLETING FORM

1. REPORT NUMBER: AFOSR-TR- 85-0694
2. GOVT ACCESSION NO.
3. RECIPIENT'S CATALOG NUMBER

4. TITLE (and Subtitle): Early Transonic Ideas in the Light of Later Developments
5. TYPE OF REPORT & PERIOD COVERED: Technical
6. PERFORMING ORG. REPORT NUMBER

7. AUTHOR(s): Julian D. Cole
8. CONTRACT OR GRANT NUMBER(s): AFOSR 82-0155

9. PERFORMING ORGANIZATION NAME AND ADDRESS:
Department of Mathematical Sciences
Rensselaer Polytechnic Institute
Troy, New York 12180-3590

10. PROGRAM ELEMENT, PROJECT, TASK AREA & WORK UNIT NUMBERS: 61102F 2304 A4

11. CONTROLLING OFFICE NAME AND ADDRESS:
AFOSR/NM
Bolling Air Force Base, DC 20332-6448

12. REPORT DATE: August 6, 1985
13. NUMBER OF PAGES: 46

14. MONITORING AGENCY NAME & ADDRESS (if different from Controlling Office)

15. SECURITY CLASS. (of this report): Unclassified
15a. DECLASSIFICATION/DOWNGRADING SCHEDULE

16. DISTRIBUTION STATEMENT (of this Report)

Approved for public release; distribution unlimited.

17. DISTRIBUTION STATEMENT (of the abstract entered in Block 20, if different from Report)

NA

18. SUPPLEMENTARY NOTES

19. KEY WORDS (Continue on reverse side if necessary and identify by block number)

Transonic
Aerodynamics

20. ABSTRACT (Continue on reverse side if necessary and identify by block number)

A survey is given of early ideas about transonic flow and their current interpretation.

DD FORM 1 JAN 73 1473 EDITION OF 1 NOV 65 IS OBSOLETE
S/N 0102-LF-014-6601

Unclassified
SECURITY CLASSIFICATION OF THIS PAGE (When Data Entered)

AD-A159 101

DTIC FILE COPY

DTIC ELECTE SEP 13 1985 D

Early Transonic Ideas in the Light of Later Developments

Julian D. Cole

Department of Mathematical Sciences
Rensselaer Polytechnic Institute
Troy, New York 12180

I. Introduction

In this lecture I am going to outline some of the early ideas about transonic flow with which Hans W. Liepmann was associated and show how they look in light of later developments.

The earliest ideas on transonic flow can be traced back to studies on gasdynamics. Chaplygin's paper[1] in 1902 treated planar gas jets by the hodograph method. Modern theoretical work connected to aeronautics dates from the papers of von Karman[2], Guderley[3], and Frankl who all derived the approximate equation of transonic flow around 1946. Early experimental work was carried out by Stack and Dryden at NASA Langley in the early '40's. Karman's paper represented the velocity potential Φ for flow past an airfoil (as in Fig. 1) as a uniform flow at the critical speed a^* plus a small disturbance $\phi(\bar{x},\bar{y})$

$$\Phi = a^* \bar{x} + \phi(\bar{x},\bar{y}) .$$

Assuming that, because of the transonic nature of the flow, $\frac{\partial}{\partial \bar{x}} >> \frac{\partial}{\partial \bar{y}}$

Karman derived the equation

$$(\gamma+1)\frac{\phi_{\bar{x}}}{a^*}\phi_{\bar{x}\bar{x}} = \phi_{\bar{y}\bar{y}} \qquad (1)$$

This basic nonlinear equation of changing type is at the heart of all transonic theory. Karman also noted the similarity parameter (effectively)

$$K = \frac{1-M_\infty^2}{\delta^{2/3}} \qquad \delta = \tau/c \ , \ M_\infty = \frac{U}{a_\infty} = \text{Mach number at infinity} = \frac{\text{flight speed}}{\text{sound speed}} \tag{2}$$

and gave scaling rules for airfoil flows. Liepmann, Ashkenas, and Cole[4] gave a more detailed derivation as well showing how including compression viscosity can yield a viscous transonic equation which can have smooth solution even when shocks are present. The shocks were shown to be thin, Re_s = Reynolds' number of the shock = 1.

Topics of considerable interest were the possibility of obtaining shock free mixed subsonic-supersonic flows by the use of the hodograph method and the physical significance of the limiting line; also the effects of the viscous boundary layer on the inviscid flow, especially in shock wave-boundary layer interactions. These are discussed below.

Another significant achievement of von Karman's was to bring Hans W. Liepmann to Caltech where he stimulated and influenced a whole generation of students and created an early interest in transonic flow.

II. Transonic Small-Disturbance Theory

The equations of transonic small-disturbance (TSD) theory can be regarded as part of systematic limit process expansion. The starting point is the Euler equation of inviscid compressible flow and the Rankine-Hugoniot jump conditions for shock waves, including the condition that the entropy increase. A typical geometry is shown (in transonic coordinates) in Fig. 2 where a vortex sheet trails downstream of the lifting wing. The asymptotic expansion has the form[5]

$$\frac{\vec{q}}{U} = (1 + \delta^{2/3} u(x,\tilde{y},\tilde{z};K) + \delta^{4/3} u_2 + \cdots) \vec{i}_x + \delta \vec{v} + \delta^{5/3} \vec{v}_2$$

$$+ \cdots, \vec{v} = (v,w) \tag{3}$$

$$\frac{p}{p_\infty} = 1 + \delta^{2/3} p + \cdots \qquad \frac{\rho}{\rho_\infty} = 1 + \delta^{2/3} \sigma + \cdots$$

The limit process has $\delta \to 0$, $M_\infty^2 = 1 - K\delta^{2/3} \to 1$ with ($x, \tilde{y} = \delta^{1/3}y$, $\tilde{z} = \delta^{1/3}z$, $K = \frac{1-M_\infty^2}{\delta^{2/3}}$ fixed). Lengths are measured in terms of the typical wing chord c. The span b should grow as $\delta \to 0$ such that $B = b\delta^{1/3}$ is fixed. Timman[6], and Krupp and Cole[7] showed how the ideas can be extended to unsteady flow with a dimensionless time coordinate

$$\tilde{t} = \frac{U}{c} \delta^{2/3} t \tag{4}$$

The representative point (x,y,z) runs far from the body as ($\delta \to 0$, $M_\infty \to 1$) for fixed $(x,\tilde{y},\tilde{z})$ to express the fact of large lateral extent of disturbances near $M_\infty = 1$. When the limit process expansion is substituted into the basic Euler system it is shown that to this order, a disturbance potential $\phi(x,\tilde{y},\tilde{z},\tilde{t})$ exists such that

$$u = \phi_x, \ \vec{v} = \tilde{\nabla}\phi, \ \tilde{\nabla} = \left(\frac{\partial}{\partial \tilde{y}}, \frac{\partial}{\partial \tilde{z}}\right) \tag{5}$$

This disturbance potential vanishes at upstream infinity and satisfies the basic TSD equation

$$(K - (\gamma+1)\phi_x)\phi_{xx} + \tilde{\nabla}^2\phi - 2\phi_{x\tilde{t}} = 0 \tag{6}$$

The pressure coefficient $c_p = \frac{p-p_\infty}{\rho_\infty U^2/2}$ is found from

$$c_p = -2\delta^{2/3}\phi_x \tag{7}$$

Some properties of the TSD equation are now summarized for steady flow in two-dimensions

$$(K - (\gamma+1)\phi_x)\phi_{xx} + \phi_{\tilde{y}\tilde{y}} = 0 \quad \text{TSD eqn.} \tag{8}$$

The equation (8) is of changing type,

elliptic if $(\gamma+1)\phi_x < K$

hyperbolic if $(\gamma+1)\phi_x > K$

with flow that is locally subsonic or supersonic respectively. $K = 0$ corresponds to sonic flow at infinity ($M_\infty = 1$). The local Mach number M_ℓ can be shown to be given by

$$K - (\gamma+1)\phi_x = \frac{1-M_\ell^2}{\delta^{2/3}}$$

The typical structure of flow at a high subsonic Mach number is shown in Fig. 3 where a local supersonic (hyperbolic) region appears over an airfoil. The supersonic region contains Mach lines or hyperbolic characteristics given by

$$\frac{d\tilde{y}}{dx} = \frac{\pm 1}{\sqrt{(\gamma+1)\phi_x - K}} \tag{9}$$

and is terminated by a shock. The shock conditions are contained in the conservation form corresponding to (8)

$$\left(K\phi_x - \frac{\gamma+1}{2}\phi^2\right)_x + (\phi_{\tilde{y}})_{\tilde{y}} = 0 \tag{10}$$

which is a version of the continuity equation. The shock is a discontinuity surface across which ϕ_x, $\phi_{\tilde{y}}$ jump. The jump conditions are given by the integrated form of (10)

$$[K\phi_x - \frac{\gamma+1}{2}\phi_x^2]d\tilde{y}_s - [\phi_{\tilde{y}}]dx_s = 0 \tag{11a}$$

and the condition that ϕ is continuous

$$[\phi] = 0 \quad \text{or} \quad [\phi_x]dx_s + [\phi_{\tilde{y}}]d\tilde{y}_s = 0 \tag{11b}$$

Here $(dx_s, d\tilde{y}_s)$ are line elements in the shock surface.

$[\ ]$ = jump = $(\ )_b - (\ )_a$, $(\ )_b$ = quantity behind shock

$(\ )_a$ = quantity ahead of shock

Further the mass flux in the x-direction.

$$\frac{\rho q_x}{\rho_\infty U} = 1 + \delta^{4/3}\left(K\phi_x - \frac{\gamma+1}{2}\phi_x^2\right) + \cdots \tag{12}$$

so that there is a maximum flux at local sonic speed (c.f. Fig. 4). The maximum of the mass flux corresponds to the fact that stream tubes have throats at local Mach number one. The TSD equations thus contain all the essential features of flow.

III. Early GALCIT Experiments

A small transonic wind tunnel 2" x 20" was constructed in 1944-5 at GALCIT by Hans W. Liepmann and a series of interesting experiments were carried out in this facility[4]. Some of these are mentioned here and some in later sections. Experiments were carried out in flow past a series of circular arc airfoils of dimensions as in Fig. 5. Surface pressure distributions were recorded and Schlieren pictures taken. Fig. 6 shows a typical pressure distribution at zero angle of attack ($\alpha = 0$). The local supersonic zone is shown clearly as is the substantial difference of the flow with laminar and turbulent boundary layers on the surface. Turbulence was induced with a trip wire. For the turbulent case in which the boundary layer is thinner the shock wave terminating the sonic region is seen clearly. These features are run also in the Schlieren photographs reproduced in Fig. 7.

IV. Numerical Methods

At the time of these experiments no reliable numerical methods existed for calculating the ideal flow, although Emmons carried out some relaxation calculations for flows with local supersonic regions. Emmons' method however

was inherently unstable and did not resolve shock waves. In the late 60's Emmons' method was revised to eliminate these drawbacks[8] and since then the method has undergone substantial development. The use of multigrids has speeded convergence and the basic ideas have been extended to the Euler equations. Here we describe the original idea and present the results of a few calculations. Finite difference methods are used to solve numerically the boundary value problem for ϕ corresponding to flow past an airfoil. The best results are obtained by using the conservative form (8)

$$\left(K\phi_x - \frac{\gamma+1}{2}\phi_x^2\right)_x + (\phi_{\tilde{y}})_{\tilde{y}} = 0 \tag{13}$$

and a corresponding conservative finite difference form. The essential boundary conditions are (i) tangent flow at the airfoil surface

$$\phi_{\tilde{y}}(x, 0\pm) = F'_{u,\ell}(x) \qquad 0 < x < 1 \tag{14}$$

where $y = \delta F_{u,\ell}(x)$ represents the upper and lower surfaces respectively (ii) vanishing of perturbations at infinity

$$\phi_x, \phi_y \to 0 \qquad \sqrt{x^2+y^2} \to \infty \tag{15}$$

(iii) Kutta condition that the flow leaves the trailing edge smoothly. In TSD this requirement is equivalent to zero pressure loading at the tail or (c.f.7)

$$\phi_x(1,0+) = \phi_x(1,0-) \tag{16}$$

The boundary value problem is shown in Fig. 8 where in addition it is noted that there is a jump in ϕ across the wake

$$[\phi] = \phi(x,0+) - \phi(x,0-) = \tilde{\Gamma} \tag{17}$$

where $\tilde{\Gamma} = \oint u\,dx + v\,d\tilde{y}$ is the circulation. It is also noted that an asymptotic

far field exists which for subsonic flow has the form of a circulation

$$\phi \sim -\frac{\tilde{\Gamma}\theta}{2\pi} + \cdots , \quad \theta = \tan^{-1} \frac{\sqrt{K}\tilde{y}}{x} \tag{18}$$

Finite difference calculations are carried out on the (i,j) mesh indicated. A conservative form is derived by considering fluxes around a central box. This reasoning is extended so that the shock waves which appear spread over three or four mesh points are consistent. For stability the difference scheme must be chosen to be type sensitive. The solutions at (i,j) can be influenced only by upstream points if the flow is locally supersonic ($\phi_x > K/(\gamma+1)$), but by both upstream and downstream points if the flow is locally subsonic. In the finite difference approximations ϕ_x at (i,j) can be calculated from a centered formula $\phi_x^{(c)}$ involving (i+1, i-1) or a backward formula $\phi_x^{(b)}$ involving (i,i-2). When these agree an (i,j) can be designated subsonic or supersonic as indicated in Fig. 9. At subsonic points (13) provides an explicit equation for ϕ_{ij} in terms of neighbors on all sides, the computational star in Fig. 9. For supersonic points however an implicit scheme is used involving only upstream points. Two other kinds of points denoted as "sonic", which applies for points near the sonic line where the flow accelerates and "shock" which applies for points where the flow decelerates to subsonic through a shock are shown.

Since the problem is non-linear the local state is not known in advance and an iteration scheme is used. At a given iteration the difference schemes are chosen and the unknowns solved for on a vertical line. Sweeps are made in the downstream direction. The analytical far field is used as a boundary condition but the value of $\tilde{\Gamma}$ is adjusted as the trailing edge is passed. To speed convergence the latest values are used whenever possible. The method converges well, gives the correct shock jumps, and for lifting cases automatically satisfies the Kutta condition.

Some results of calculations are shown in Fig. 10 and 11 for a parabolic arc airfoil[9] and a NACA 0012[10]. For the first the sonic line and shock appear as well as the surface pressure. Figure 12[9] shows the flow field features for a higher freestream Mach number where the main shock has moved aft of the airfoil and a fishtail shock pattern appears.

V. Shock-free Supercritical Flows

The possibility of shock free flows past airfoils with local supersonic regions was of considerable interest in the early days of transonic research. This was stimulated by Ringleb's exact hodograph solution[11], analogous to incompressible flow around a half-plane, which has a smooth transonic region. Experimentally it was possible to produce a small shock-free supersonic zone in the flow around a simple shape. For example see Fig. 13 where some of Liepmann's results are reproduced[4].

Other exact solutions, analytical and numerical, were derived from hodograph considerations and gave shock free flow past special airfoil shapes. The hodograph equations are linear so that solutions can be obtained and the airfoil shape found later. For the TSD system the hodograph equations are obtained by a direct interchange of dependent and independent variables. Rewrite (8) as the system

$$\begin{cases} ww_x = \nu\tilde{y} \\ w_{\tilde{y}} = \nu_x \end{cases} \tag{19}$$

where

$$w = (\gamma+1)\phi_x - K \ , \ \nu = (\gamma+1)\phi_{\tilde{y}}$$

Then

$$\begin{cases} w\tilde{y}_\nu = x_w \\ x_\nu = \tilde{y}w \end{cases} \tag{20}$$

since $w_x = \frac{1}{j}\tilde{y}_\nu$ etc, and J = Jacobian = $\frac{\partial(x,\tilde{y})}{\partial(w,\nu)}$. From this, it is seen

that the approximate stream function $\tilde{y}(w,\nu)$ is given by a solution of Tricomi's equation.

$$w\tilde{y}_{\nu\nu} - \tilde{y}_{ww} = 0 \tag{21}$$

This is the simplest linear equation of mixed type, elliptic in the subsonic region $w < 0$, hyperbolic in the supersonic region $w > 0$. The exact potential equation can be transformed in a similar way to produce Chaplygin's equation which has properties analogous to (21).

Some special exact solutions for mixed flow past an airfoil were given by Tomotika and Tamada[12]. Recent advances have been the work of Nieuwland[13] which used Chaplygin functions to represent analytically families of airfoils and Garabedian and Korn[14] who use a finite-difference hodograph method to obtain numerical solutions of airfoil flows. The latter employ real characteristics in the hyperbolic region and complex characateristics in the elliptic region and a sufficient number of parameters to generate families of shapes with local subsonic zones. A typical airfoil and its pressure distribution in shock free flow is shown in Fig. 14. The pressure distribution is also calculated according to TSD theory with a fully conservative relaxation scheme (FCR) as described in Sec. IV and a non-conservative scheme (NCR)[15], as well as a calculation of Garabedian, Korn & Jameson[16]. The drag coefficient, which is theoretically zero (see next section) is evaluated on several different control surfaces[15].

The smooth hodograph solutions are seen to be isolated solutions since a smooth mixed flow can not be found when the boundary conditions in the physical plane change slightly (Morawetz[17]). An early paper of Guderley[18] suggests a singularity of a perturbation in the downstream corner of the sonic region. They are isolated solutions in the same sense as the famous Busemann supersonic biplane. When the conditions are changed slightly a neighboring solution is found with a shock wave. An example of the calculation of such a flow appears in

Fig. 15, where the shock wave is apparent. Experiments verify these features.

Guderley[3] suggests that the shocks in the local supersonic region are initiated by an envelope formation of the compressive reflection of Mach lines from the sonic line. A detailed look at the calculations of Fig. 10 verify this idea[9]. Thus a shock free airfoil is one in which the shape of the sonic line is just right so that no envelope is formed.

VI. Shock Waves and Drag

The connection of shock waves and drag was made explicit by Liepmann[19] in 1950 with a study of linearized supersonic flow past an airfoil. By considering the weak shock waves in such a flow a correction to the Mach angle was made for shock angle and location and the formula was found

$$\text{Drag/(length)} = \rho_\infty T_\infty \int_{\text{shocks}} [S]dy \tag{22}$$

where [S] = jump in specific entropy across a shock wave. Drag is related directly to entropy production. Similar results appear later in works by von Karman[20] and Oswatitsch[21].

Analogous considerations apply to TSD flow. Germain[22] gave a derivation of a drag formula for TSD theory starting from a local conservation law in two-dimensions. The generalization to three-dimensional flow was given in[5] and reads

$$\left(K\frac{u^2}{2} - \frac{v^2+w^2}{2} - \frac{\gamma+1}{3}u^3\right)_x + (uv)_{\tilde{y}} + (uw)_{\tilde{z}} = 0 \tag{23}$$

This conservation law easily follows from the three-dimensional version of (8) and the equation of irrotationality. The values of (uv) on $\tilde{y} = 0$ are proportional to the incremental drag for a planar system since the pressure increment is proportional to u and the wing slope to v. Integration of (23) over

a control surface as shown in Fig. 16 yields a formula for drag. Since (23) is not a physical global conservation law it is not conserved across shock waves. Letting the control surface grow to infinity contributions from the shock and vortex sheet remain. The result is

$$\tilde{D} = \frac{\text{Drag}}{\rho_\infty U^2 \delta^{4/3} c^2} = \lim_{x\to\infty} \underbrace{\int\int_{-\infty}^{\infty} \left(\frac{v^2+w^2}{2}\right) d\tilde{y}\, d\tilde{z}}_{\text{vortex drag}} - \underbrace{\frac{\gamma+1}{12} \int\int [u]^3 d\tilde{y}\, d\tilde{z}}_{\text{shocks}} \tag{24}$$

The first term of (24) is the familiar expression for vortex drag in terms of the kinetic energy in the wake while the second term, the wave drag is a scaled version of the Liepmann formula. $[u]$ is the jump of ϕ_x across the shock and the entropy change is proportional to $[u]^3$. Thermodynamic considerations for weak shocks show.

$$\frac{\gamma+1}{12} \int\int_{\text{shocks}} [u]^3 d\tilde{y}\, d\tilde{z} \sim \rho_\infty T_\infty \int\int_{\text{shocks}} [S] dy\, dz \tag{25}$$

It should be noted that these simple results do not carry over for stronger shocks. The drag-entropy formula (24) can be used to provide a check on the consistency of numerical TSD calculations[15]. In Fig. (17) the shock and flow field for a parabolic arc at $M_\infty = .909$ is shown. The $\int [u]^3 d\tilde{y} - \int [c_p]^3 d\tilde{y}$ is plotted also and the drag coefficient is computed both from the surface pressure integral and the entropy jump. The result is

$$\begin{aligned} C_D &= .0315 \quad \text{surface pressure integration} \\ C_D &= .0320 \quad \text{shock entropy integration} \end{aligned} \tag{26}$$

Careful calculations of TSD flow enable the wave drag to be found. An example of an application is the flow past an NACA 64A010 airfoil in a slotted wall wind-tunnel. The drag rise due to shock wave formation (C_{D_0} = friction drag) is fairly well represented. See Fig. 18.

VII. Sonic Flow and the Law of Stabilization

The flow at $M_\infty = 1$ has a special structure elucidated first by Guderley and Frankl. In order to understand this flow consider first the sequence of flow patterns past an airfoil or body at free stream Mach numbers close to one, Fig. 19. At high subsonic Mach numbers a large supersonic zone is formed terminated by an oblique shock near the trailing edge and the fishtail shock, as calculated in Fig. 12. At $M_\infty = 1$, the supersonic zone in the sequence of steady flows grows to infinity and the fishtail shock goes to downstream infinity. A limit characteristic or Mach wave appears which is asymptotically parallel to both the sonic line and the tail shock at infinity. This limit characteristic divides the flow field into an upstream and downstream part. Any (infinitesimal) disturbance in the flow, in the supersonic region, for example, can send a disturbance downstream which eventually reaches the sonic line and affects the entire subsonic region. Any disturbance originating downstream of the limit characteristic can not affect the upstream flow. The flow in the upstream section up to the limit characteristic thus has an elliptic nature and must be calculated all at once. It is effectively independent of the flow downstream of this characteristic. Downstream of the limit characteristic the flow can, for example, be calculated as in a hyperbolic region by the method of characteristics. When the free stream becomes slightly supersonic a detached shock wave which has subsonic flow behind near the axis ($\tilde{y}=0$) appears ahead of the body. The flow becomes supersonic near the airfoil and terminates again in an oblique tail shock. It can thus be noted that the flow in the neighborhood of the body does not change qualitatively very much since the oncoming flow is always close to a uniform subsonic flow.

For $M_\infty = 1$, the far-field is a similarity solution. With $K = 0$ (8) becomes, for the planar case

$$(\gamma+1)\phi_x\phi_{xx} - \phi_{\tilde{y}\tilde{y}} = 0 \qquad (27)$$

The far-field can be thought of as being produced by a singularity at the origin and, due to non-linearity, represented in the form

$$(\gamma+1)\phi(x,\tilde{y}) = \tilde{y}^{3\kappa-2}\, f(\xi;\kappa),\ \xi = \frac{x}{\tilde{y}^{\kappa}} \tag{28}$$

a one-parameter family of similarity solutions. Thus note

$$(\gamma+1)\phi_x = \tilde{y}^{2\kappa-2}\ f'(\xi)\ ,\ (\gamma+1)\phi_{xx} = \tilde{y}^{\kappa-2}\ f''(\xi) \tag{29}$$

$f(\xi;\kappa)$ is thus found from

$$(f'-\kappa^2\xi^2)f'' - 5\kappa(1-\kappa)\xi f' + 3(1-\kappa)(3\kappa-2)f=0, \quad -\infty < \xi < \xi_L \tag{30}$$

The coordinates are illustrated in Fig. 20. The flow must start at infinity decelerating and spreading around the body, then accelerate through sonic and smoothly through the limit characteristic. It can be seen from (29) that the sonic line ($f'=0$) as well as the limit characteristic and tail shock must lie on similarity curves ξ,ξ_L, and ξ_S respectively. The characteristic condition (+) (29) becomes

$$f'(\xi_L) = \kappa^2\xi_L^2 \tag{31}$$

ϕ also must be symmetric in $\tilde{y}$, the apparent thickness effect dominating the flow at infinity. This occurs because both acceleration and deceleration of a sonic flow produces a widening of stream tubes (cf Fig. 4). One constant of integration remains if integration is started at $\xi = -\infty$ and two conditions must be satisfied at the limit characteristic if $f''(\xi_L)$ is to be finite. Thus the solution exists only for a special of κ. Guderley showed from the hodograph solution that

$$\kappa = \frac{4}{5} \quad \text{planar case} \tag{32}$$

and by numerical integration that $\kappa = \frac{4}{7}$ for the analogous axisymmetric case. The latter result was shown to be exact by various writers e.g.[23]. Eqn. (30) has a group property so that the solution can be written

$$f(\xi) = \frac{1}{A^3} F(A\xi), \quad A = \text{const.} \tag{33}$$

The scale factor A depends on the size (and shape) of the body. Thus the far-field can be standardized to have $\xi_L = 1$. By considering shock jumps the solution can be continued to downstream infinity. A particularly useful representation of the solution was given parametrically by Frankl[24]

$$\begin{aligned} f(s) &= a_1^{3/5} s^{-1/5} \left(1 - \frac{s}{2} + \frac{s^3}{3}\right), \quad a_1 = \frac{2^9 3^3}{5^5} \\ \xi(s) &= a_1^{1/5} s^{-2/5} \left(s - \frac{1}{2}\right) \end{aligned} \tag{34}$$

where the following relationships are noted

ξ	$-\infty$	0	ξ^*	$\xi_L = 1$	ξ_s
s	0	$\frac{1}{2}$	1	4/3	$\frac{1}{6}(5\sqrt{3} + 8)$

(35)

Frankl produced this result by clever observations about special hodograph solutions; an analogous result has been derived by inspection in the axisymmetric case.

A useful extension of the far-field (28) is to regard it as the first term of an expansion of the form

$$(\gamma+1)\phi(x,\tilde{y}) = \tilde{y}^{2/5} \left[\frac{1}{A^3} f(A\xi) + C_0 \tilde{y}^{\sigma_0} \frac{f_0(A\xi)}{A^3} + C_1 \tilde{y}^{\sigma_1} \frac{f_1(A\xi)}{A^3} \right] \tag{36}$$

valid as $\tilde{y} \to \infty$ for ξ fixed. The perturbation functions $f_i = g$, $i = 0, 1$ satisfy the variational equation (with $\sigma_i = \alpha$)

$$(f' - \frac{16}{25}\xi^2)g'' + (f'' + \frac{4}{5}(2\alpha - \frac{9}{5})\xi)g' - \alpha(\alpha - 1)g = 0 \tag{37}$$

If $g = s^{-\alpha/2} h(t)$, $t = \frac{3}{4} s$ (37) becomes a standard hypergeometric equation

$$t(1-t)h'' + (\frac{1}{2} - \frac{1}{3}(5\alpha + 4)t)h' + \frac{5}{12}\alpha(5\alpha - 2)h = 0 \tag{38}$$

in the interval $\begin{pmatrix} -\infty \leq \xi \leq \xi_L = 1 \\ 0 \leq t \leq 1 \end{pmatrix}$. The two linearly independent solutions around $t = 0$ are

$$\begin{aligned} h_I &= F(\tfrac{5}{2}\alpha, \tfrac{1}{6}(2-5\alpha); \tfrac{1}{2}; t) \\ h_{II} &= t^{\frac{1}{2}} F(\tfrac{1}{2}(5\alpha+1), \tfrac{5}{6}(1-\alpha); \tfrac{3}{2}; t) \end{aligned} \tag{39}$$

Thus solutions smooth on passing through the limit characteristic are given by the spectrum

$$\sigma_i : \cdots -\frac{3}{5}, -\frac{2}{5}, -\frac{1}{5}, 0, \frac{2}{5}, \frac{8}{5}, \frac{11}{5}, \frac{14}{5} \cdots \tag{40}$$

For the expansion near infinity $\sigma_0 = 0$, $\sigma_1 = -\frac{1}{5}$ and the f_i are simple functions.

The solutions just discussed can be used to relate a flow with a free-stream Mach number close to one to that at Mach number one. In TSP form this relates a flow with small $|K|$ to that with $K = 0$. For flow subsonic at infinity the dominant term in the far-field is the circulation term, basically the solution which decays most slowly for

$$K\phi_{xx} + \phi_{yy} = 0 \ , \ \phi \to -\frac{\tilde{\Gamma}}{2\pi}\Theta \tag{41}$$

But for $K = 0$ the far-field is given by (26) with $\kappa = \frac{4}{5}$. Thus there is a non-uniformity at infinity of $\phi(x,\tilde{y};K)$ as $K \to 0$ and inner and outer expansions are

needed. For the inner expansion valid near the airfoil the first term is sonic flow past the airfoil and corrections are sought. In early work Liepmann and Bryson[25] proposed that at $M_\infty = 1$ the local Mach number on a body does not change as the free stream Mach number changes near one because of the qualitative ideas outlined above. The Law of Stabilization proposed by Ryzhov and Lipschitz[26] and the more detailed work of Cook and Ziegler[27] following the method of matched asymptotic expansion indicated in[28] give a deeper and more precise description of this Mach number freeze. The starting point is a solution at $M_\infty = 1$ and several are available, for example, for a wedge Guderley and Yoshihara[3] gave the result while Tse[29] worked out lifting airfoils at $M_\infty = 1$. Both of these methods rely on a hodograph formulation. Let $\phi^*(x,\tilde{y})$ represent the sonic flow past an airfoil with the far-field (28). Then the flow for $K > 0$ is represented as an inner expansion, generated from a limit process $K \to 0$, $x,\tilde{y}$ fixed.

$$\phi(x,\tilde{y};K) = \phi^*(x,\tilde{y}) + K\frac{x}{\gamma+1} + \varepsilon(K)\,\phi_c\,(x,\tilde{y}) + \cdots \tag{42}$$

$\varepsilon(K)$ is the order of magnitude of the correction which is sought and $\phi_c(x,\tilde{y})$ is the correction potential. $\phi^*(x,\tilde{y})$ satisifes the sonic TSD eqn (25) and its boundary conditions while $\phi_c(x,\tilde{y})$ is found from the variational equation

$$(\gamma+1)(\phi^*_x\,\phi_{c_{xx}} + \phi^*_{xx}\,\phi_{c_x}) - \phi_{c_{yy}} = 0 \tag{43}$$

The expansion (42) is not valid near infinity so that an outer expansion in rescaled variables is sought

$$\phi(x,\tilde{y};K) = \sigma(K)\,\bar{\phi}(\bar{x},\bar{y}) + \cdots \tag{44}$$

The associated limit process has $\bar{x},\bar{y}$ fixed as $K \to 0$, $x,\tilde{y} \to \infty$, that is

$$\bar{x} = \mu(K)x, \quad \bar{y} = \nu(K)\tilde{y} \qquad \mu, \nu \to 0.$$

The condition that the rescaled equation be subsonic at infinity but still nonlinear and of changing type produces a one parameter family of flows.

$$\phi(x,\tilde{y};K) = \frac{K}{\mu(K)}\,\bar{\phi}(\bar{x},\bar{y}) + \cdots, \text{ with } \nu = \mu\sqrt{K} \tag{45}$$

with the resulting version of the TSD equation

$$(1 - (\gamma+1)\bar{\phi}_x)\bar{\phi}_{xx} + \bar{\phi}_{yy} = 0 \tag{46}$$

The inner and outer expansions must match and in a simple way as $x,\tilde{y} \to \infty$, $\bar{x},\bar{y} \to 0$. ϕ^* is defined along similarity curves which then must match

$$\xi = \frac{x}{\tilde{y}^{4/5}} = \frac{K^{2/5}}{\mu^{1/5}}\,\frac{\bar{x}}{\bar{y}^{4/5}} = \bar{\xi}\,.$$

Thus $\mu = K^2$, $\bar{x} = K^2 x, \bar{y} = K^{5/2}\tilde{y}$. The general form of the flow as it looks in outer variables is shown in Fig. 21. Higher terms in the flow near infinity for the inner and the flow near the origin in the outer expansion (42),(45) then depend on the spectrum associated with (37).

These expansions can then be written (with the scale factor A = 1)

$$\phi(x,\tilde{y};K) = \frac{1}{\gamma+1}\left\{\tilde{y}^{2/5}\ f(\xi) + c_0 + \tilde{y}^{-1/5}\ f_1(\xi) + \cdots\right\} + \frac{Kx}{\gamma+1}$$
$$+ \varepsilon(K)\phi_c(x,\tilde{y}) + \cdots \tag{47a}$$
$$\text{inner}$$

$$= \frac{1}{K}\ \frac{1}{\gamma+1}\left\{\bar{y}^{\,2/5}\ f(\bar{\xi}) + \bar{x}\ + C_1\,\bar{y}^{\,8/5}\bar{f}1(\bar{\xi}) + \cdots\right\}, \text{ outer} \tag{47b}$$

A comparison of these two as $\bar{x},\bar{y} \to 0$, $x,\tilde{y} \to \infty$ along similarity curves shows that $\phi_1(x,\tilde{y})$ has similarity form at infinity and that

$$\epsilon(K) = K^3 = \frac{(1-M_\infty^2)^3}{\delta^2} \qquad (48)$$

This weak dependence on deviation from $M_\infty = 1$, for the potential and pressure distribution is the essential part of the law of stabilization. The term $K \frac{x}{\gamma+1}$ in these expansions represents the change of the flow at infinity and adds a constant pressure level to the solution. Germain[22] derived a conservation law formula for the scale factor A relating it to properties of the solution (not known in advance) on the body surface. Cook and Ziegler[27] have extended these ideas to find C_1. The boundary value problem for the inner correction solution is sketched in Fig. 22. An empirical fit of the Law of Stabilization to some experimental drag measurements of Vincenti[30] is drawn in Fig.22.

VIII. Concluding Remarks

TSD theory ard calculations have made great studies in the last 35 years based on the work of the pioneers. The understanding of the physical phenomena that has been thus achieved enables us to go forward with more elaborate calculations and including more physical effects. One can only admire the deep insight of the early workers in this area such as H.W. Liepmann.

"Research sponsored by the Air Force Office of Scientific Research, Air Force Systems Command, USAF, under Contract/Grant No. AFOSR-82-0155. The United States Government is authorized to reproduce and distribute reprints for Governmental purposes notwithstanding any copyright notation thereon."

References

1. Chaplygin, S.A. On Gas Jets (1902) Collected Works. v. II Government Press. 1948 (Russian).
2. von Karman, T. The Similarity Law of Transonic Flow. J. of Math. and Physics v. 26 No. 3, Oct. 1947, pp. 182-190.
3. Guderley, K.G. Theorie Schallnahe Stromungen, Springer-Verlag. Berlin 1957, English Translation Addison Wesley 1962.
4. Liepmann, H.W., Ashkenas H., and Cole, J.D. Experiments in Transonic Flow. USAF TR 5667, Wright-Patterson AFB, 1948.
5. Cole, J.D. Twenty Years of Transonic Flow. Boeing Scientific Research Laboratories, D1-82-0878, July 1969.
6. Timman, R. Unsteady Motion in Transonic Flow. Symposium Transsonicum Aachen 1962, Springer (K. Oswatitsch ed.), pp. 394-401.
7. Krupp, J.A., and Cole, J.D. Unsteady Transonic Flow Studies in Transonic Flow IV, UCLA Eng. 76104, Oct. 1976.
8. Murman, E.M., and Cole, J.D. Calculation of Plane Steady Transonic Flows. AIAA J. v. 9, No. 1, Jan. 1971, pp. 121-141.
9. Murman, E.M. Analysis of Embedded Shock Waves Calculated by Relaxation Methods. AIAA J. v. 12, No. 5, May 1974, pp. 626-632.
10. Small, R.D. Numerical Solutions for Transonic Flows, Part 1. Plane Steady Flow over Lifting Airfoils, TAE Rept. 273, Technion, Dept. of Aero. Eng. Haifa, 1976.
11. Ringleb, F. Exakte Losungen der Differentialgleichungen einer adiabatischen Gasstromung ZAMM v. 20, 1940, pp. 185-198.
12. Tomotika, S., and Tamada, K. Studies on Two Dimensional Transonic Flows of Compressible Fluids, Parts I,II,III. Q. Appl. Math. v. 127, 1950, p. 127, p. 381, v. 129, 1951, p. 129, (72,272).

References (continued)

13. Nieuwland, G.Y. Transonic Potential Flow around a Family of Quasi-elliptical Aerofoil Sections NLR Tech. Rept. R172, 1967, Amsterdam.

14. Garabedian, P., and Korn, D. Numerical Design of Transonic Airfoils, Numerical Solutions of Partial Differential Equations II. Academic Press, 1971.

15. Murman, E.M., and Cole, J.D. Inviscid Drag at Transonic Speeds Studies in Transonic Flow III. UCLA Eng. 7603, Dec. 1975.

16. Garabedian, P.R., and Korn, D.G. Analysis of Transonic Airfoils Comm. Pure and Appl. Math. v. 24, 1971, pp. 841-851. See also Jameson, A., Gruman Aero. Rept. 390-71-1.

17. Morawetz, C. On the Non-existence of Continuous Transonic Flows past Profiles I. Comm. Pure and Appl. Math. v. 9(1956), pp. 45-68, II v. 10(1957) pp. 107-131.

18. Guderley, G. On the Presence of Shocks in Mixed Subsonic-Supersonic Flow Patterns.
Advances in Applied Mechanics v. III, 1953, pp. 145-184.

19. Liepmann, H.W. On the Relation between Wave Drag and Entropy Increase., Douglas Aircraft Co., Rept. SM13726, 1950.

20. von Karman, T. On the Foundation of High Speed Aerodynamics and Jet Propulsion VI, pp. 3-30, Princeton University
Press 1957 (Sears, W. R. ed.)

21. Oswatitsch, K. Gas Dynamics. 1956, Academic Press.

22. Germain, P. Ecoulements Transsoniques Homogenes ONERA T.P. 242, 1965. Also appears in Progress in Aero. Sci. v. 5, Pergamon Press, 1964.

23. Muller, E.A., and Matschat, K. Ahnlichkeitslosungen der Transsonischen Gleichungen bei der Anstrom-Machzahl 1, Proc. 11th Int. Cong. Appl. Mech., Munich, 1964, pp. 1061-8, Springer.

References (continued)

24. Landau, L.D. and Lifshitz, E.M. Fluid Mechanics (English edition) 1959, Pergamon Press.

25. Liepmann, H.W. and Bryson, Jr., A.E. Transonic Flow past Wedge Sections J. Aero. Sci. v. 17, 1950, pp. 745-755.

26. Lipschitz, Yu. B., and Ryzhov, O. Transonic Flow around a Carrying Profile, Fluid Dynamics v. 13 No. 1, 1971, pp. 78-84 (English translation from Russian).

27. Cook, L.P., and Ziegler, F. The Stabilization Law of Transonic Flow. To appear S.I.A.M. J. Appl. Math.

28. Cole, J.D. Asymptotic Problems in Transonic Flow, AIAA paper, 82-0104, 1982.

29. Tse, E. Airfoils at Sonic Velocity Ph.D. thesis, University of California, Los Angeles 1981.

30. Vincenti, W.G., Dugan, D.W., and Phelps, E.R. An Experimental Study of the Lift and Pressure Distribution on a Double Wedge Profile at Mach Number near Shock Attachment NACA TN 3225, 1954.

Figure Titles

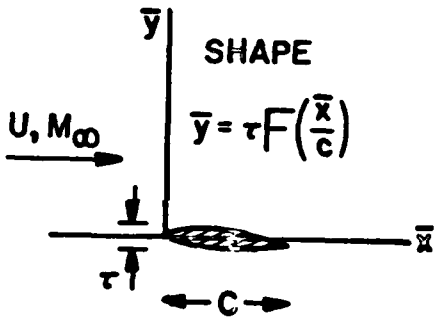
$\bar{y}$
SHAPE
$\bar{y} = \tau F\left(\frac{\bar{x}}{c}\right)$
U, M_∞
$\bar{x}$
τ
c

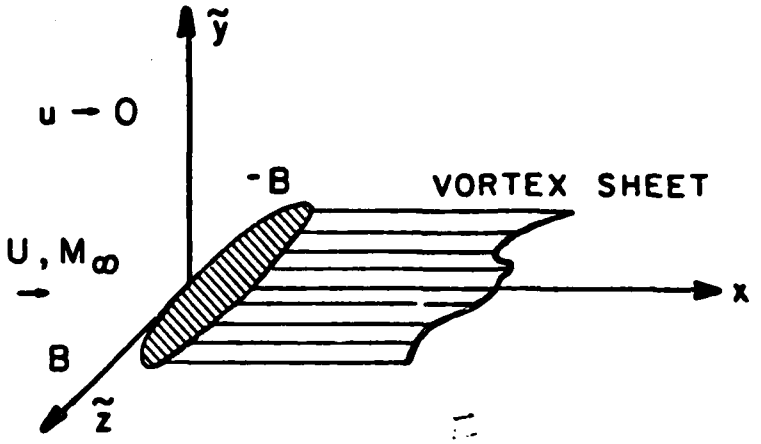
$\tilde{y}$
u → 0
-B
VORTEX SHEET
U, M_∞
x
B
$\tilde{z}$

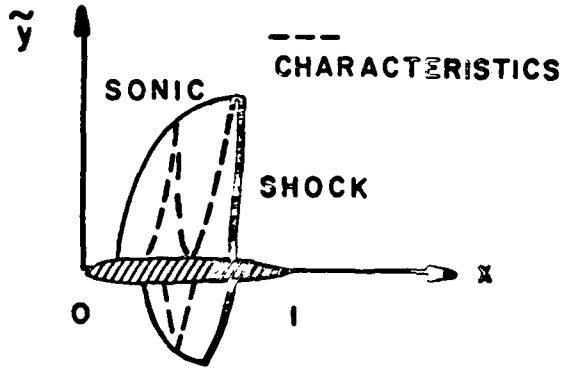
ỹ
CHARACTERISTICS
SONIC
SHOCK
x
0
1

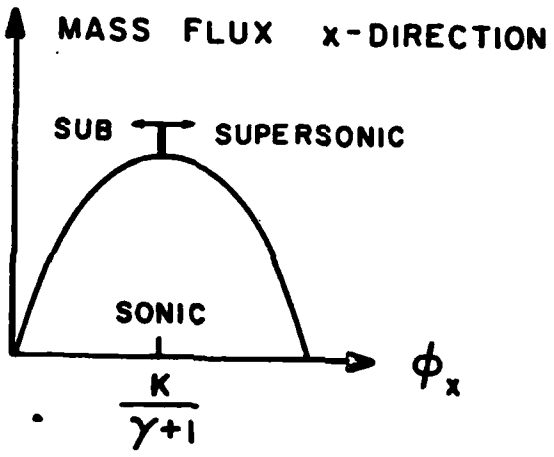
MASS FLUX x-DIRECTION
SUB
SUPERSONIC
SONIC
ϕ_x
$\frac{K}{\gamma+1}$

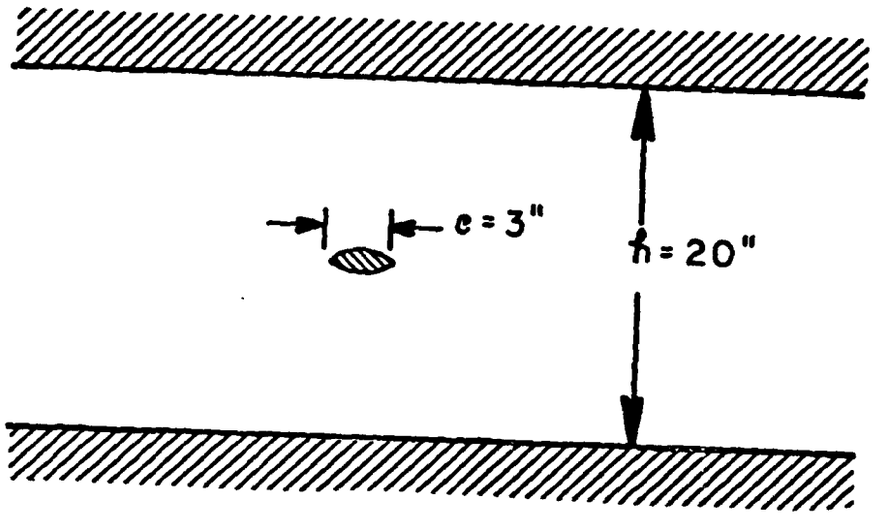

F -

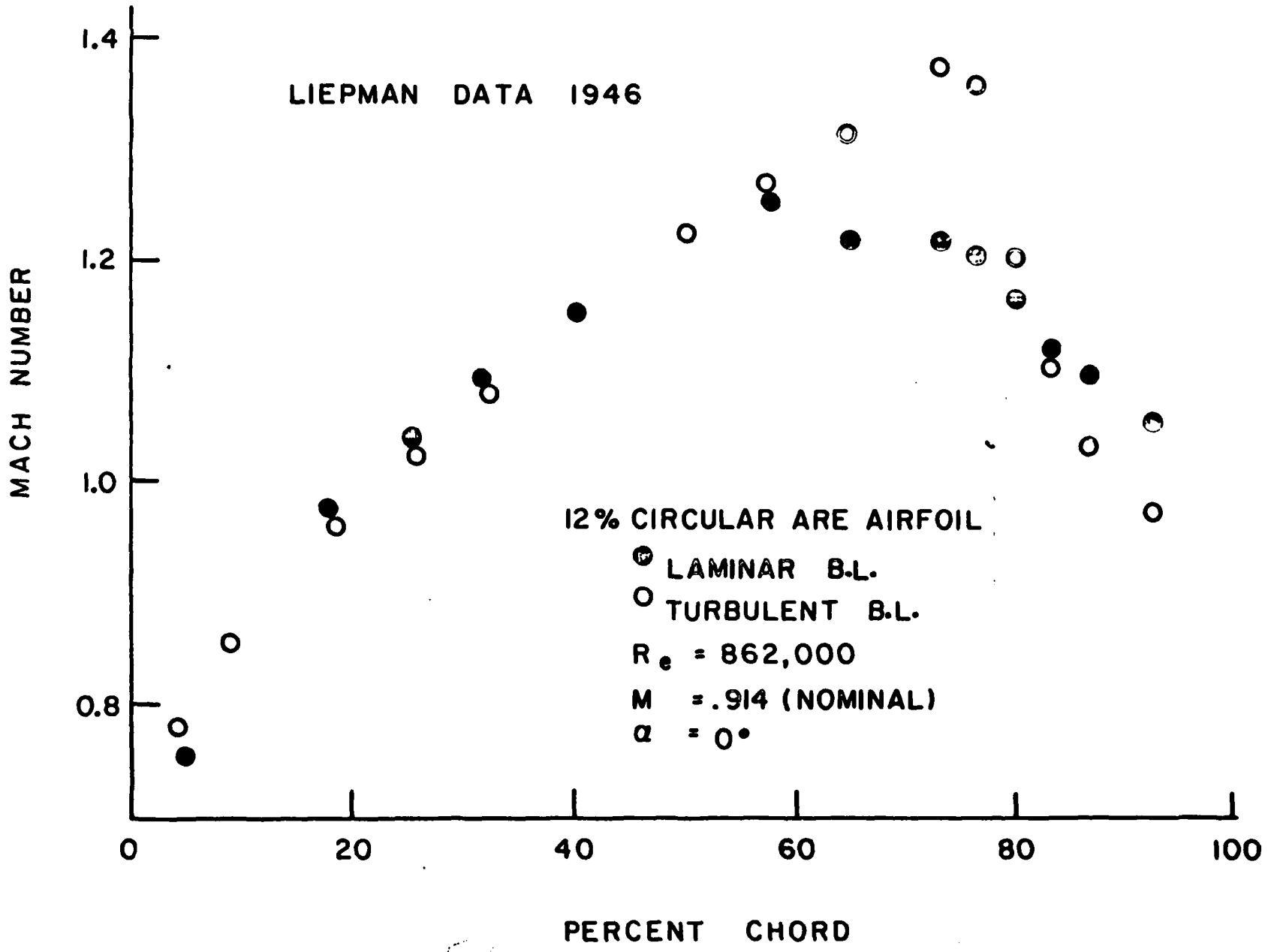
LIEPMAN DATA 1946
MACH NUMBER
1.4
1.2
1.0
0.8
0
20
40
60
80
100
PERCENT CHORD
12% CIRCULAR ARE AIRFOIL
LAMINAR B.L.
TURBULENT B.L.
R_e = 862,000
M = .914 (NOMINAL)
α = 0°

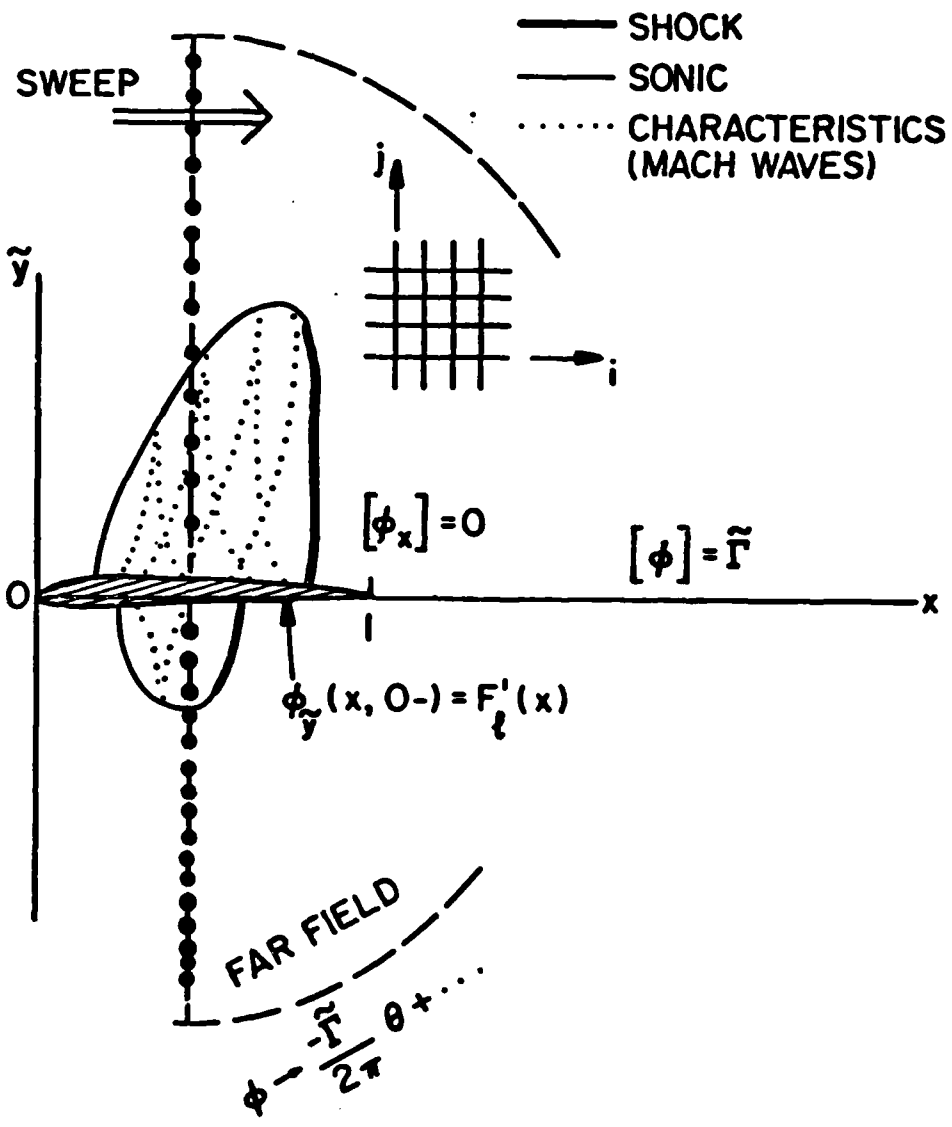
SHOCK
SONIC
CHARACTERISTICS
(MACH WAVES)
SWEEP
j
i
$\tilde{y}$
$[\phi_x] = 0$
$[\phi] = \tilde{\Gamma}$
0
1
x
$\phi_{\tilde{y}}(x, 0-) = F_\ell'(x)$
FAR FIELD
$\phi \sim \frac{-\tilde{\Gamma}}{2\pi}\theta + \cdots$

$\phi_x^{(c)}$	$\phi_x^{(b)}$	TYPE	STAR
<	<	ELLIPTIC (SUB)	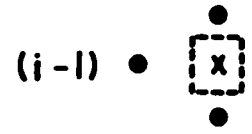
>	>	HYPERBOLIC (SUPER)	
>	<	SONIC	
<	>	SHOCK PT. (STRONG)	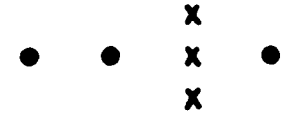

RESULTS

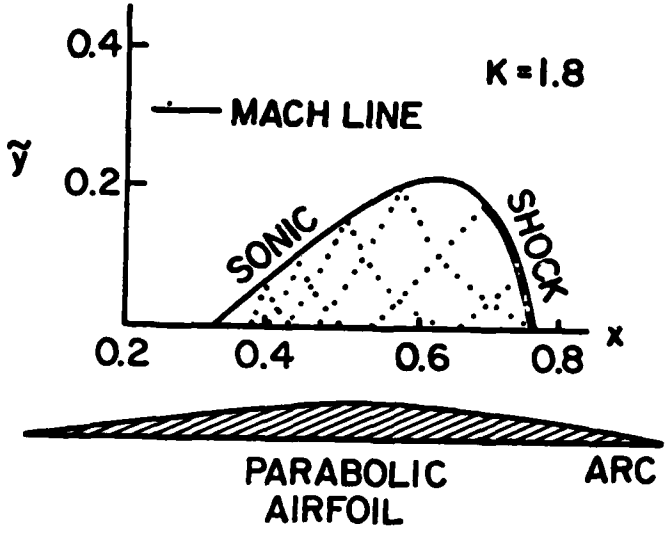
0.4
0.2
$\tilde{y}$
K = 1.8
MACH LINE
SONIC
SHOCK
0.2
0.4
0.6
0.8
x
PARABOLIC
AIRFOIL
ARC

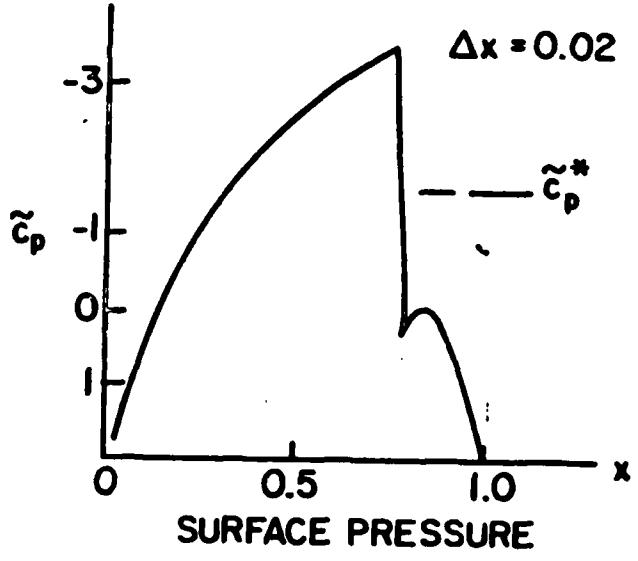
Δx = 0.02
-3
-1
0
1
$\tilde{c}_p$
$\tilde{c}_p^*$
0
0.5
1.0
x
SURFACE PRESSURE

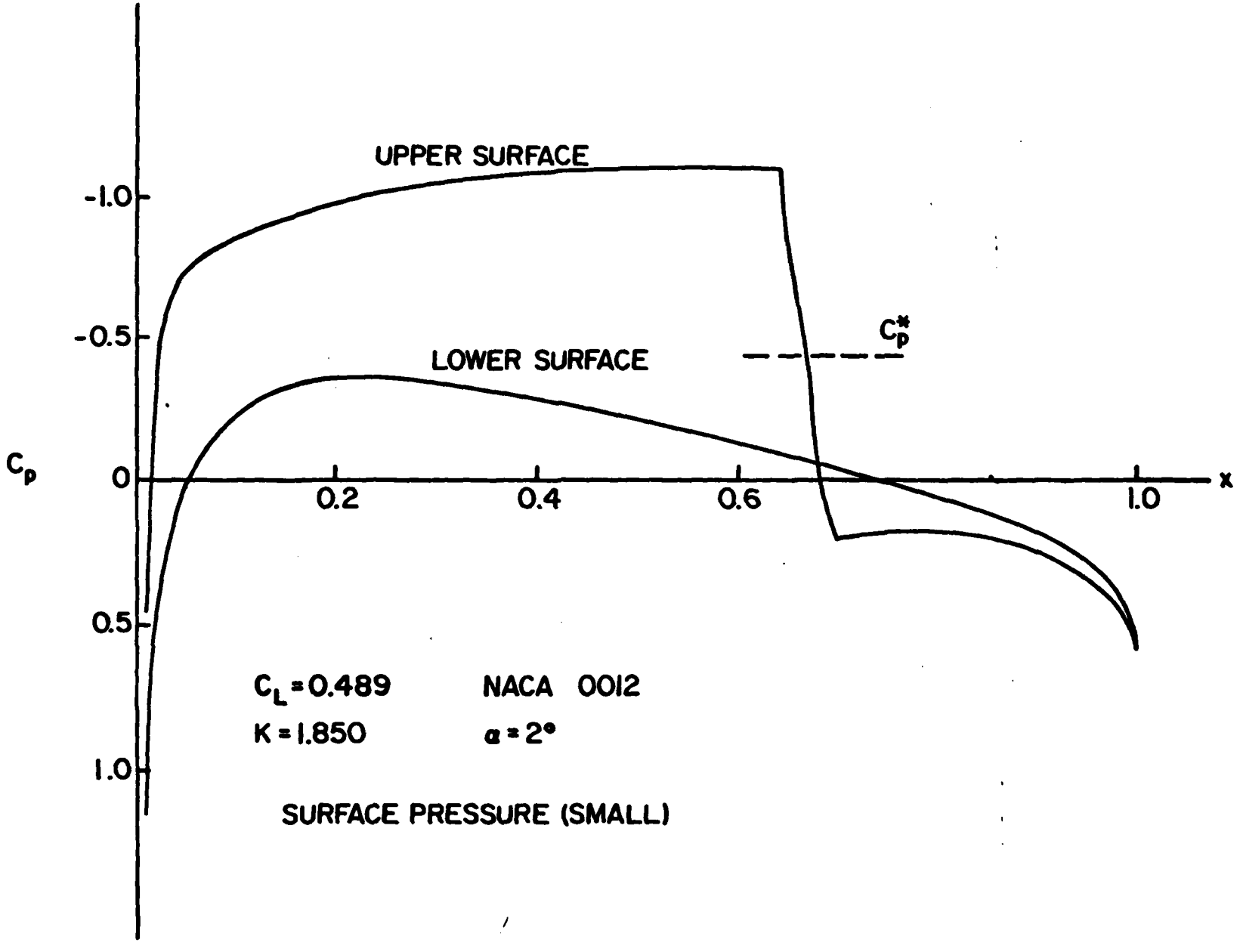

SURFACE PRESSURE (SMALL)

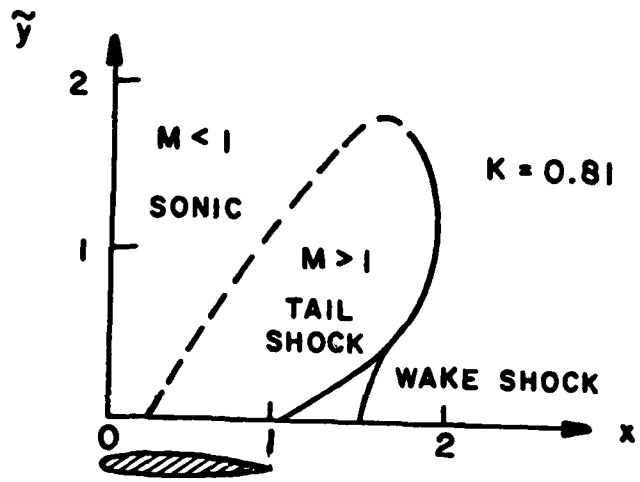

FLOW FIELD FEATURES - PARABOLIC ARC

SHOCK FREE FLOW

LIEPMANN DATA 1946

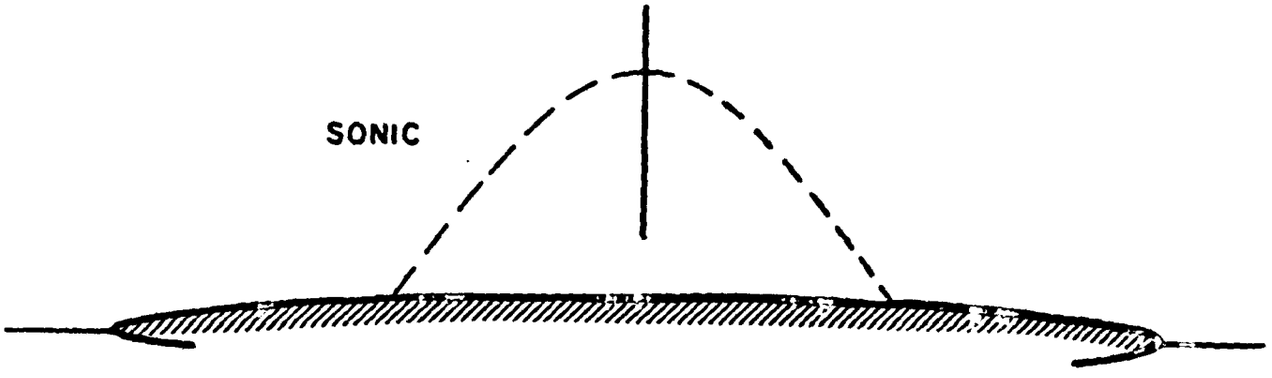

SHAPE OF SUPERSONIC ZONE 6% CIRCULAR ARC

M_{∞} = 1.084 TURBULENT B. L.

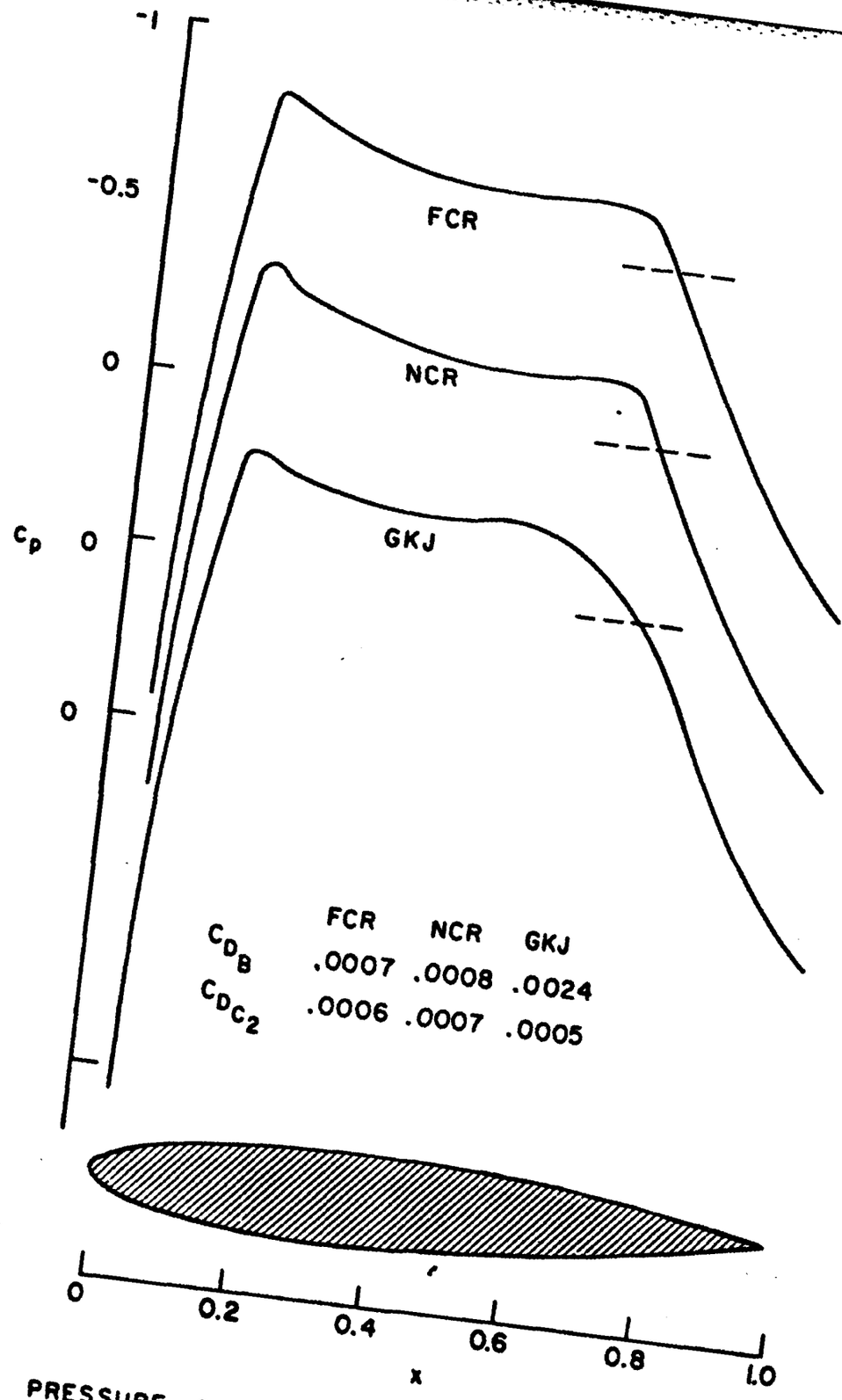

PRESSURE DISTRIBUTION AND DRAG COEFFICIENTS FOR KORN AIRFOIL AT DESIGN CONDITIONS

$M_\infty = 0.80$, $\alpha = 0°$

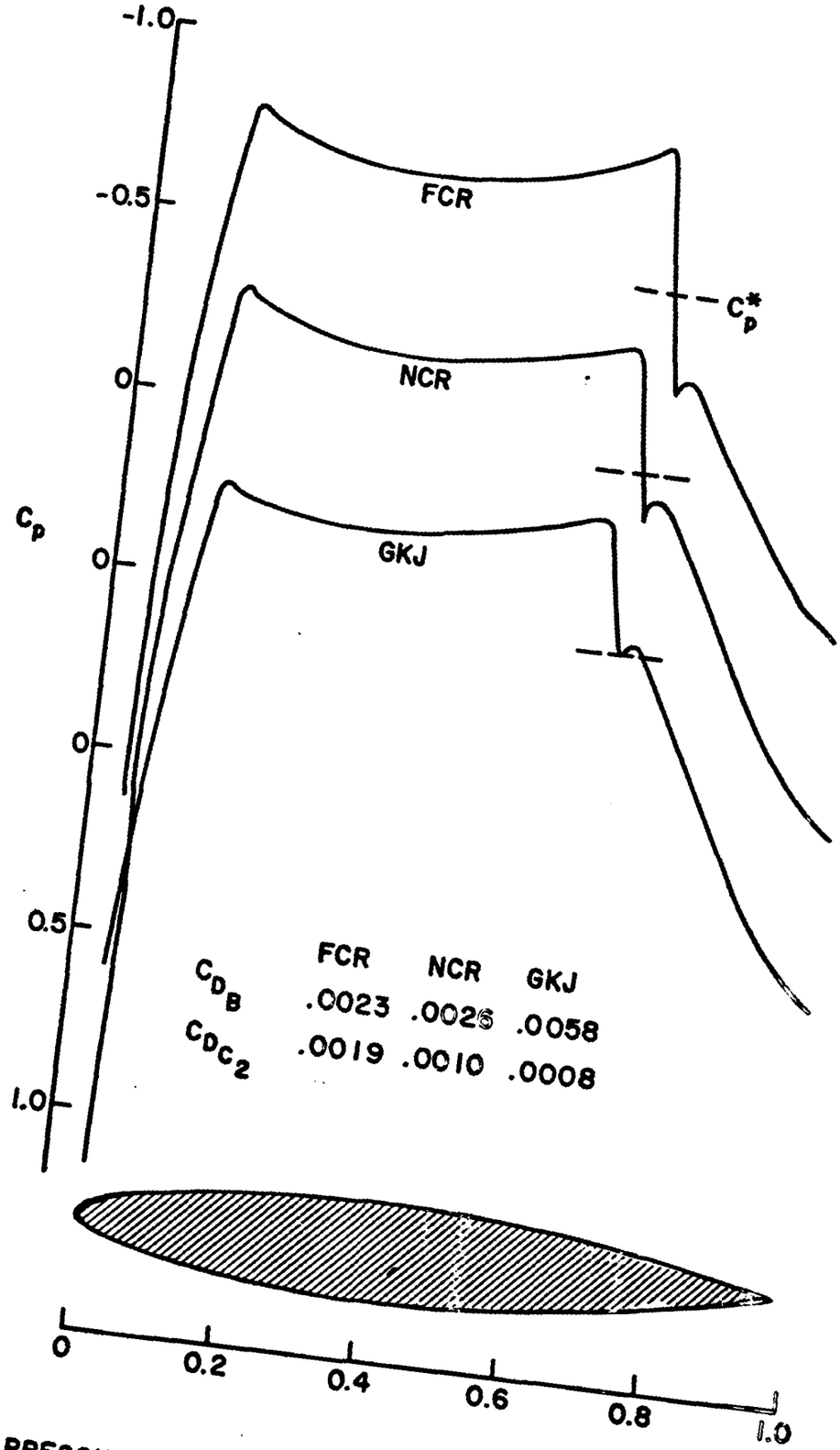

PRESSURE DISTRIBUTION AND DRAG COEFFICIENTS FOR KORN AIRFOIL AT OFF DESIGN CONDITION

$M_\infty = 0.81$, $\alpha = 0°$

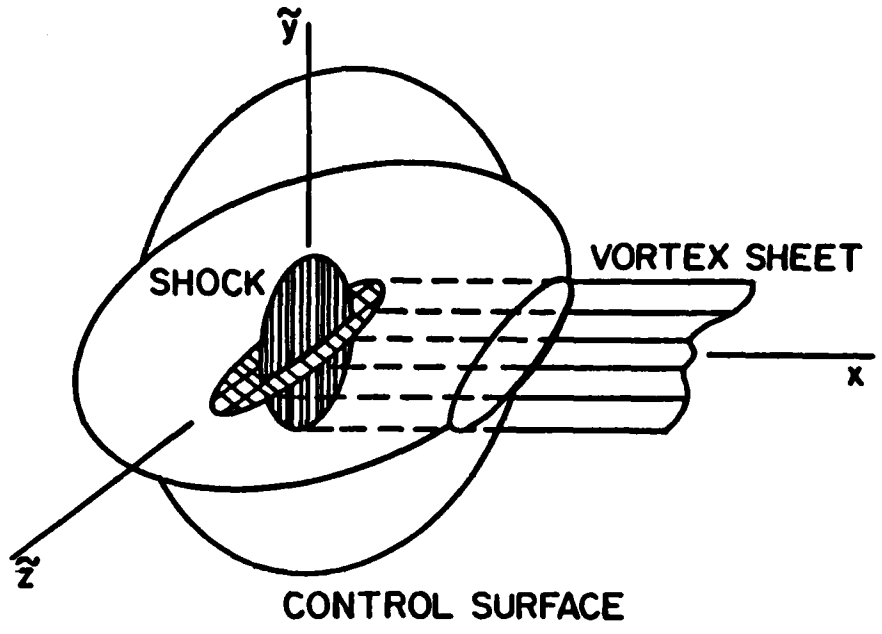
$\tilde{y}$
SHOCK
VORTEX SHEET
x
$\tilde{z}$
CONTROL SURFACE

DRAG RESULTS

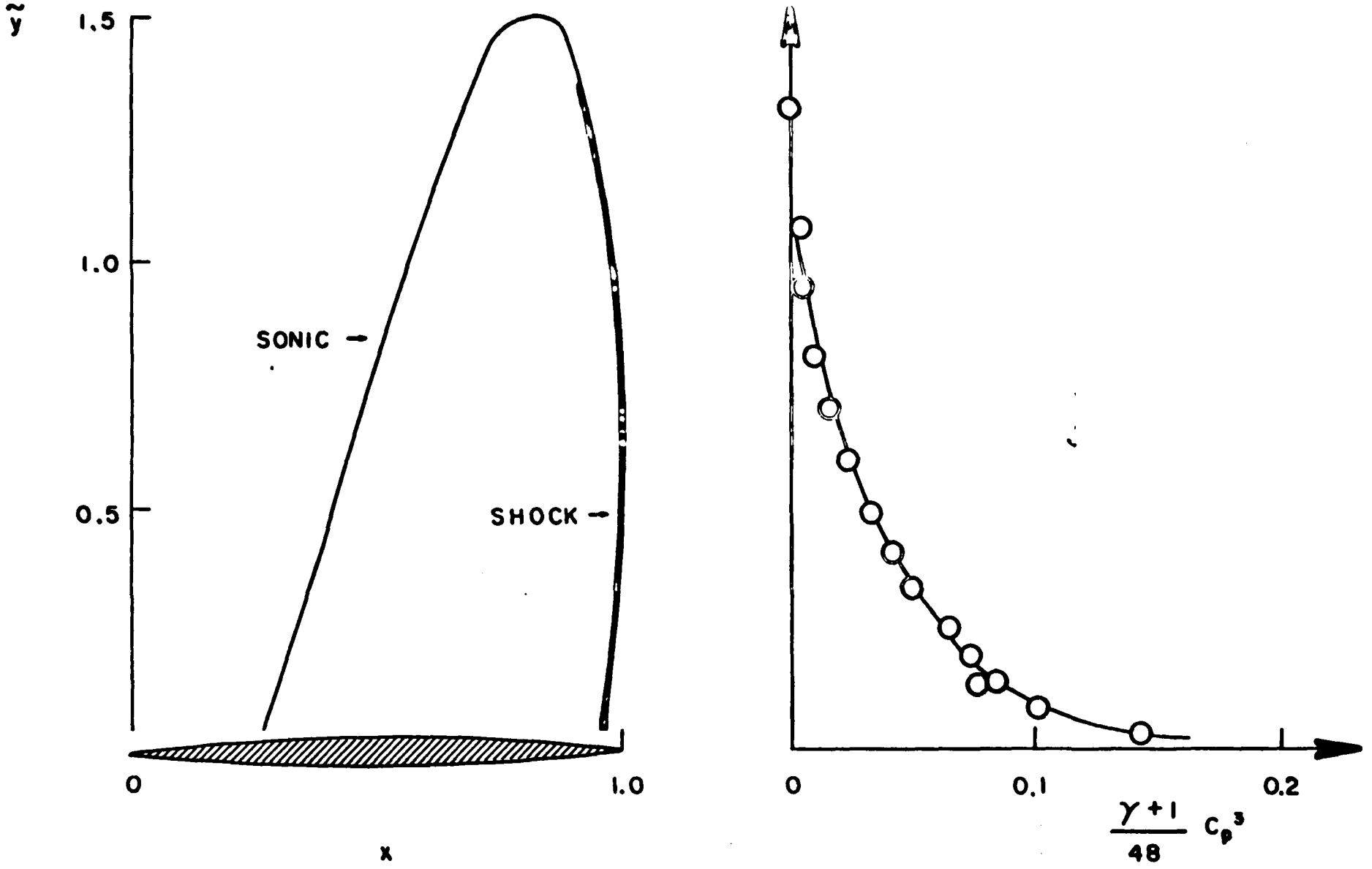

PARABOLIC ARC
C_D = 0.0315
C_D = 0.0320

M_∞ = 0.909
(SURFACE PRESSURE)
(SHOCK INTEGRATION)

DRAG COMPARISON WITH EXPERIMENTS

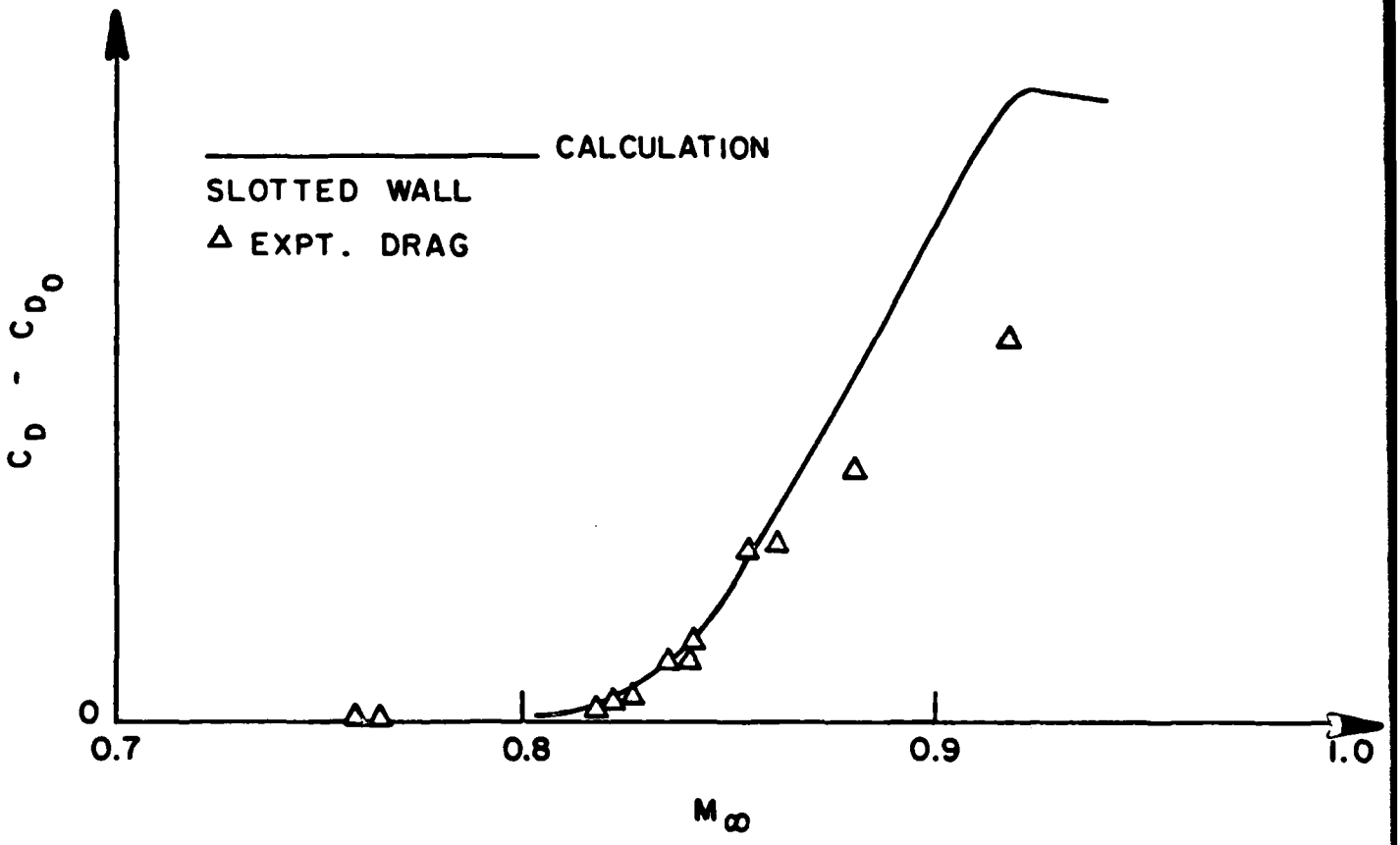

64A010 AIRFOIL

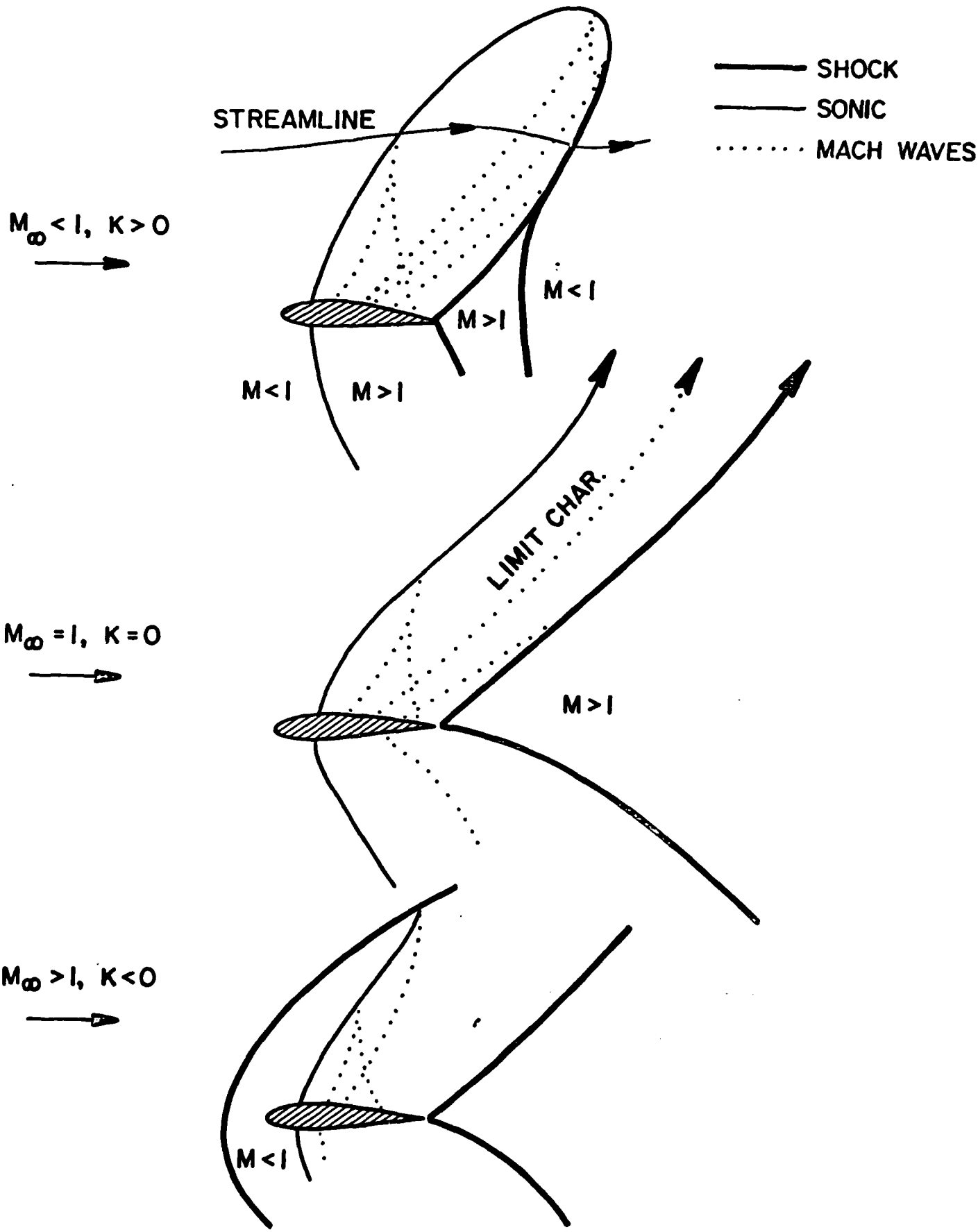
SHOCK
SONIC
MACH WAVES
STREAMLINE
$M_\infty < 1,\ K > 0$
M<1
M>1
M<1
M>1
LIMIT CHAR.
$M_\infty = 1,\ K = 0$
M>1
$M_\infty > 1,\ K < 0$
M<1

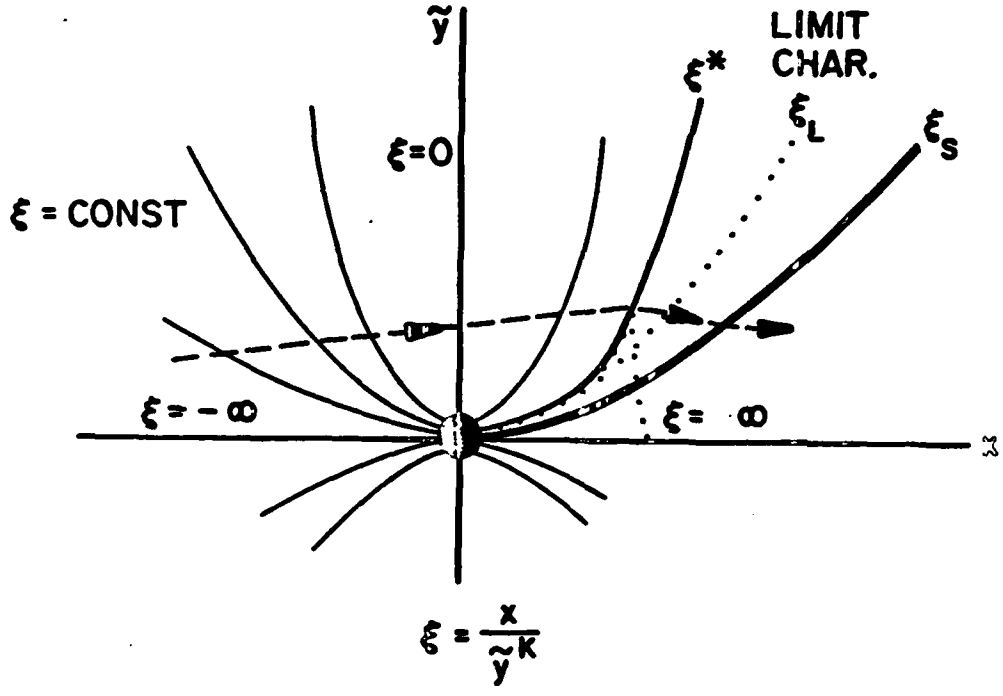
$\tilde{y}$
LIMIT
CHAR.
ξ^*
ξ_L
ξ_S
$\xi=0$
ξ = CONST
$\xi = -\infty$
$\xi = \infty$
x
$\xi = \frac{x}{\tilde{y}^K}$

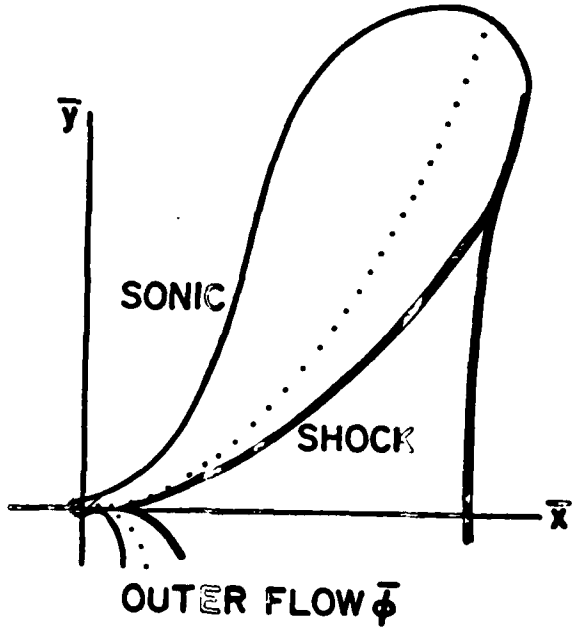
$\bar{y}$
SONIC
SHOCK
$\bar{x}$
OUTER FLOW $\bar{\phi}$

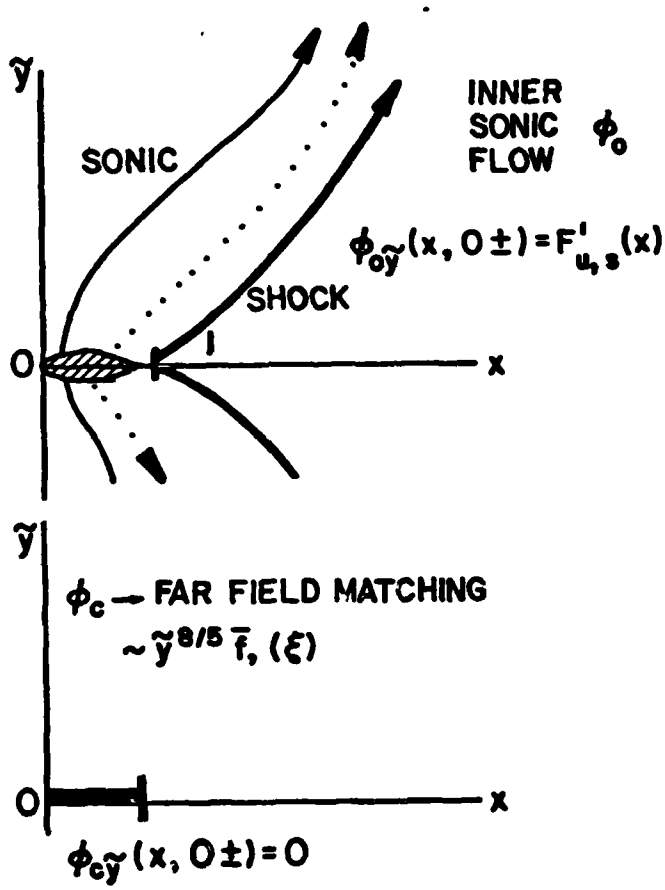
$\tilde{y}$
SONIC
INNER
SONIC
FLOW
ϕ_o
$\phi_{o\tilde{y}}(x, 0\pm) = F'_{u,s}(x)$
SHOCK
1
0
x
$\tilde{y}$
ϕ_c — FAR FIELD MATCHING
$\sim \tilde{y}^{8/5} \bar{f}, (\xi)$
0
x
$\phi_{c\tilde{y}}(x, 0\pm) = 0$

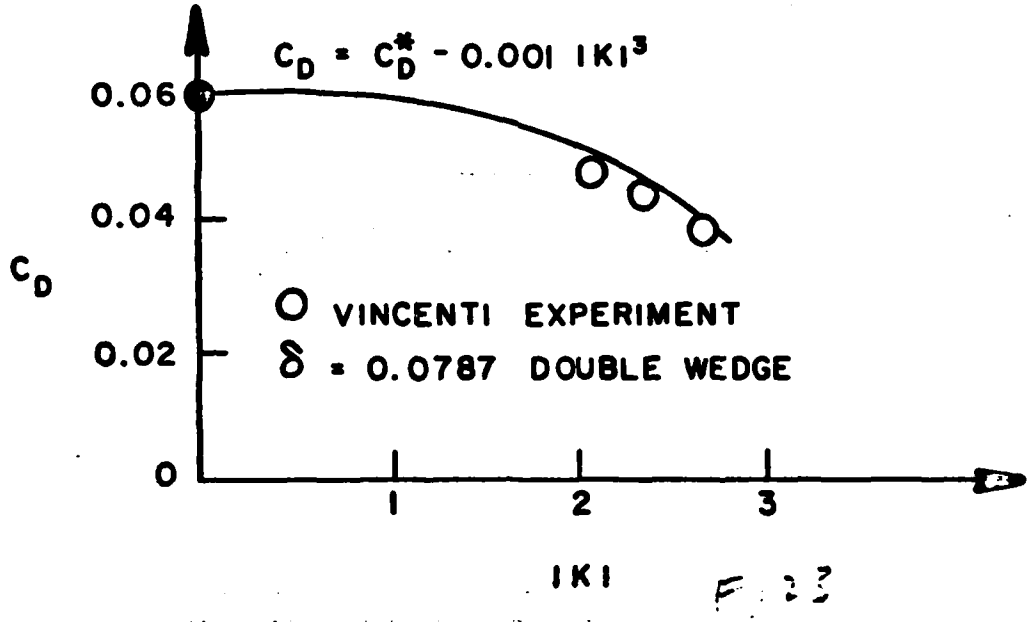
$C_D = C_D^* - 0.001\ |K|^3$
0.06
0.04
C_D
0.02
0
O VINCENTI EXPERIMENT
δ = 0.0787 DOUBLE WEDGE
1
2
3
|K|

F 2.3

END

FILMED

11-85

DTIC